SSRG International Journal of Electrical and Electronics Engineering
ISSN: 2348-8379/ https://doi.org/10.14445/23488379/IJEEE-V12I3P108

Volume 12 Issue 3, 74-83, March 2025

Original Article

Hybrid Optimization of Unified Power Quality Conditioner Placement for Enhanced Grid Performance

G. Lakshminarayana[1*], D. Rene Dev[2], K. Vijetha[3], Neha Verma Gour[4], R. Mageswaran[5], S. Sree Dharinya[6]

[1]*Department of Electrical and Electronics Engineering, VNR Vignana Jyothi Institute of Engineering and Technology, Hyderabad, Telangana, India.*
[2]*Department of Electrical and Electronics Engineering, MVJ College of Engineering, Bengaluru, Karnataka, India.*
[3,4]*Department of Electrical Engineering, Medicaps University, Indore, Madhya Pradesh, India.*
[5]*Department of Electrical and Electronics Engineering, S.A. Engineering College, Thiruverkadu, Chennai, Tamilnadu, India*
[6]*School of Computer Science Engineering and Information Systems, Department of Software and Systems Engineering, VIT University, Vellore, Tamilnadu, India.*

**Corresponding Author : glngitam@gmail.com*

Received: 27 September 2024 Revised: 18 December 2024 Accepted: 03 March 2025 Published: 31 March 2025

Abstract *- In response, this research paper introduces an innovative approach for enhancing power quality and stability in electrical grids by optimally placing Unified Power Quality Conditioner (UPQC) devices. The proposed methodology leverages the synergies of a Hybrid Genetic Algorithm based Chaotic Dragonfly Optimization (HGACDO) to determine the most effective locations for UPQC installation. The Genetic Algorithm (GA) brings powerful exploration capabilities, simulating natural selection to refine potential solutions. This is combined with the Chaotic Dragonfly Optimization's (CDO) efficient global search mechanism inspired by the brood parasitism behaviour of cuckoos. This synergy results in the HGACDO method, which is uniquely tailored for optimal UPQC allocation. The proposed approach not only considers the technical aspects of UPQC placement but also considers the cost-effectiveness, power losses and voltage stability index. By fusing GA and CDO, the HGACDO algorithm enables a comprehensive exploration of solution spaces, enhancing the precision of UPQC placement. To validate the effectiveness of the HGACDO model, extensive testing is conducted on benchmark IEEE 69 and IEEE 33 test bus systems. The results demonstrate significant improvements in power quality, stability and operational efficiency. Through its innovative hybridization, the HGACDO method emerges as a promising avenue for achieving optimal UPQC allocation, thereby advancing the reliability and performance of modern power systems.*

Keywords *- Hybrid Genetic Algorithm based Chaotic Dragonfly Optimization (HGACDO), IEEE 69, 1EEE 33 test bus, Optimal placement, UPQC system.*

1. Introduction

Technology advancements have led to increased use of FACTS devices for reactive power and voltage regulation in steady state network operating situations. Two voltage-sourced converters make up the basic architecture of UPQC. On their DC sides, these converters are coupled to one another and connected to the AC system via shunt and series transformer compensators [1-3]. UPFC compares to a system with an ideal series voltage source and an ideal shunt current source in terms of its ability to regulate flicker, active, voltage sag, harmonics, dynamic, and reactive power. To ensure that incoming current to the PCC bus is managed sinusoidally, the UPQC shunt section integrates current to PCC simultaneously. Most UPQC assessments concentrate on UPQC performance and operate with two bus distribution systems in a dynamic, short-term manner [4-6]. Several researches have been published regarding the optimal placement of UPQC power systems. However, these methods have some limitations, which are discussed below. A strategy for continuous operation optimization for Open UPQC for energy loss. The idea of minimizing distribution networks is put forth in [7]. Implementing each of the planning situations can significantly lower the yearly energy loss. However, this requires more DSTATCOM and will improve the overall VA rating. Combining the Lion and Crow Search Algorithms has been proposed for the optimal size and location of UPQC in the distribution network [8]. High convergence and better PQ are present. However, factors affecting power quality, such as UPQC costs, power loss, and the Voltage Stability Index (VSI), are not examined or taken into account. Optimal management and architecture are proposed in [9] to carry out UPQC using the parameter phase angle regulation approach. The smooth transition of displacement angle throughout the transient state can be ensured by implementing the suggested

control mechanism. Nevertheless, during UPQC compensatory operation, VA loadings will not be greater than VA ratings. Effective UPQC and DG Positioning in the Radial Distribution System is covered in [10]. Here, line losses are decreased, and VP is enhanced more successfully. However, for the best distribution of UPQC and DG, optimization techniques must be utilized. Based on operational forecasting in a distribution grid with dispersed generators, optimum location and capacity design for UPQCs have been presented in [11]. The associated dispatching techniques show that they are preferable in terms of variability in voltage and line loss. However, because voltage fluctuations appear and only last for a short amount of time, UPQC mostly operates in reactive power correction mode. Reference [12] discusses the placement of open UPQC and optimum sizing in distribution networks considering load expansion. The findings suggest that the provided design technique performs well in terms of economic and technical aspects and is valuable for network designers. However, installing more SHUs in the network incurs maintenance costs and higher installation, resulting in a higher value. The most appropriate position for UPQC to enhance power quality is suggested in [13] for the 14 bus distribution network. A key factor in quickly restoring the voltage is the UPQC's ideal position. However, unplanned outages carried on by significant failures impair the stability of the electrical distribution system.

The best UPQC placement and size for enhancing power system quality have been suggested in [14]. The SS-CSA technology has achieved a function of reduced cost. Nevertheless, as the total amount of UPQC ascends, so do their installation costs. A realistic distributing system for executing the Bacterial Foraging Algorithm Inspired Model for UPQC Positioning has been presented in [15]. Reactive power compensation issues in actual networks of distribution are able to be handled by this technique. To solve difficulties with reactive power compensation, a modern algorithm based on swarms of natural creatures must be used. It has been mentioned in [16] to use the Moth Flame Optimisation (MFO) technique for UPQC placement. Utilizing MFO, the optimal position and complicated voltage supplied by the UPQC's series compensator is determined. Nevertheless, the MFO struggles to strike a good equilibrium between exploration and exploitation, and there is minimal information sharing among people. Hence, this work proposes a hybrid optimization model for optimal UPQC positioning and sizing. The proposed work's key contribution is summed up as follows:

- To maximize the power quality, stability and operational efficiency of the electrical grids by optimizing the placement of UPQC devices.
- To design a novel methodology named Hybrid Genetic Algorithm based Chaotic Dragonfly Optimization (HGACDO), which leverages the strengths of both Genetic Algorithm (GA) and Chaotic Dragonfly Optimization (CDO) to determine optimal UPQC installation locations.
- To simulate the performance and effectiveness of the HGACDO model through Matlab with extensive testing on benchmark IEEE 33 and IEEE 69 test bus systems.

2. Analytical Model Optimal Placement and Sizing of UPQC Power System

2.1. Objective Model

The UPQC positioning is the key component of the specified PQ enhancement. The PQ improvement goals need to be satisfied by the UPQC placement. Equation (1) illustrates the structure of the established objective function. Power loss is shown in Equation (5), where the loss is specified. In this case, O_k denotes the electrical conductivity of the kth line connecting the i and j buses. δ_i and $\delta_j$stand for the voltage angle of the i and j buses, respectively. In Equation (3), the $UPQC_{cost}$ is specified. Here, R stands for the property's rate of exchange, O represents UPQC's operational boundaries in MVAr, $UPQC_{cost}$ stands for investing cost, $UPQC_{Cost_{year}}$ stands for the UPQC's annual cost and mUPQC and corresponds to the UPQC's resilience. In Equation (4), the VSI notion is illustrated. In Equation (4), μ stands for the tiny constant, which represents the voltage for the b^{th} bus. The VSI is required to be between 0.9 and 1.1, and if it shows any deviation from this range, a penalty has been placed.

$$OB = min(UPQC\ cos\ t + P_{Loss} + Voltage\ Stability\ Index \quad (1)$$

$$UPQC_{Cost}\left(US\left(\frac{\$}{kVAr}\right)\right) = 0.003O^2 - 0.2691O + 188.22 \quad (2)$$

$$UPQC_{Cost_{year}} = UPQC_{cost}\frac{(1-R)^{mUPQC}\times R}{(1+R)^{mUPQC}-1} \quad (3)$$

$$VSI = \begin{cases} 1 & if\ V^{min} \le V^b \le V^{max} \\ exp(\mu|1-V^b|) & otherwise \end{cases} \quad (4)$$

$$P_{Loss} = \sum_{k=1}^{N_L} P_{Lossk} = \sum_{k=1}^{N_L} O_k \{V_i^2 + V_j^2 - 2V_iV_j\ cos(\delta_i - \delta_j)\} \quad (5)$$

The following section explains the way particular metrics of equality and inequality are required to be fulfilled with the chosen design.

2.2. Equality Constraints

The magnitude of bus voltage and the phase angle are in relation to reactive and active line power. Finally, Equation (6) depicts the distribution system's active power balance, while Equation (7) shows the reactive power balance.

$$P_{H_i} - P_{E_i} - \sum_{k=1}^{N_L} O_{ik}\{V_i^2 + V_j^2 - 2V_iV_j\cos(\delta_i - \delta_j)\} = 0 \quad (6)$$

$$QU_{H_i} - QU_{E_i} - \sum_{k=1}^{N_L} P_{ik}\{V_i^2 + V_j^2 - 2V_iV_j \sin(\delta_i - \delta_j)\} = 0 \quad (7)$$

Here, $P_{E_i}$and P_{H_i} specify the active power supplied according to the system's active power demand and the bus in sequence. The term P_{Loss} stands for overall active power loss. Reactive power that has been introduced at the ith bus has been referred to by the symbols QU_{H_i}, $QU_{E_i}$and Q_{Loss}, while reactive power loss is designated byQ_{Loss}. The i and j are connected among susceptance and conductance, indicated by the symbols P_{i-j} and O_{i-j} correspondingly. Both the i and j buses' voltage magnitudes are specified by the symbols $V_i$and V_j.

2.3. Inequality Constraints

The capabilities and operating boundaries of the system are influenced by these qualities.

Limit of a line flow: This limit denotes the maximum power that can be sent across a specific transmission line when certain predetermined conditions are met. The limits depend on stability or thermal considerations. Equation (8) illustrates the power flow limit factor, where SE_kmax signifies the largest value of power flow via the k^{th}line.

$$SE_k \leq SE_k \max \quad (8)$$

Limit of a Bus voltage: Voltage magnitude limits and voltage imbalance limit nodes are described in connection to bus voltage limitations, respectively. Radial Distribution System's coverage of effective UPQC and DG Positioning

$$V^{min} < V < V^{max} \quad (9)$$

2.4. Modelling of UPQC

A three-phase, four-wire voltage source converter-based device called UPQC is depicted in Figure 1. In real, UPQC is modelled using Active Power Filters (APF) in both series and shunt configurations. All current-related difficulties, including load imbalance compensation, reactive power compensation, DC link voltage management, power factor improvement, and current harmonic compensation, are all addressed by connecting a shunt APF over the loads. A 3-phase sequential transformer connects the series APF to a network. This serves as a regulated voltage source that may mitigate and regulate voltage for any voltage-related issues, including flicker, voltage harmonics, etc. The load disturbance region is converted into a normal operation zone by UPQC through fault assurance. The actual power loss, as well as the voltage sag and imbalance, has decreased. Utilized are two inverters linked by an individual DC storage capacitor. In this paper, one inverter is used to put in a shunt current, while the following one is utilized to inject a series voltage. The amount of inserted voltage via the series inverter V_{se} depends primarily on the largest voltage sag, which needs to be reduced. This is exactly what shunt inverters and series inverters perform. The supply voltage magnitude is specified as $V_s = kV_{SO}$ and $V_s = V_{SO}$, where $k_{sag} = (1 - k)$.for both voltage sag and normal circumstances. $V_L = V_{SO} = V_s$ at any state load voltage, and according to Equation (10), the required series voltage insertion for attenuating voltage sag at the voltage sag point is computed. Active power retrieved from the source through seamless UPQC is used to indicate active power required by the load. A source current is provided as in Equation (11), where I_L and I_s denote load current and compensated source end current, respectively. In this sense, $kV_sI_s = V_LI_L \cos\varphi$. Equations (10) and (11), respectively, provide the Volt Amperes (VA) rating of a series inverter.

$$V_{se} = \sqrt{V_L^2 + (kV_{SO})^2 - 2V(kV_{SO})\cos\delta} = V_s\sqrt{1 + k^2 - 2k\cos\delta} \quad (10)$$

$$I_s = I_L \cos {}^{\varphi}/_{k} \quad (11)$$

$$SE_{se} = V_{se}I_s = V_sI_L \cos\varphi\sqrt{1 + k^2 - 2k\cos {}^{\delta}/_{k}} \quad (12)$$

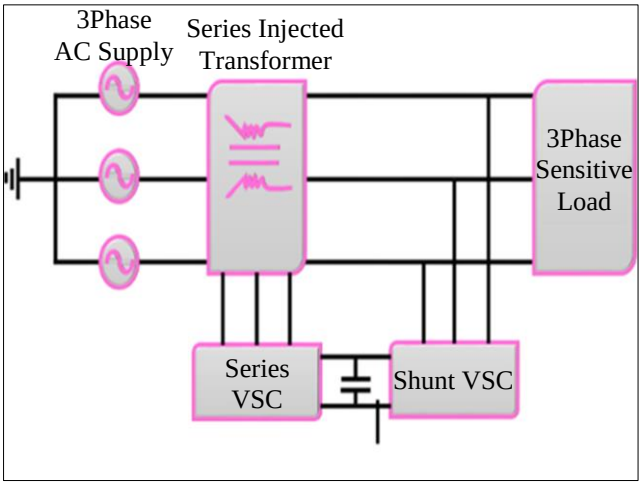

Fig. 1 Pictorial representation of UPQC

Reactive and active power transmitted by a series inverter is represented by Equations (13) and (14) correspondingly, where$\theta_{se} = 180^o - tan^{-1}(sin\,\delta/1 - cos\delta)$.

$$P_{se} = SE_{se}\cos\theta_{se} \quad (13)$$

$$QU_{se} = SE_{se}\,sin\,\theta_{se} \quad (14)$$

According to Equation (15), the word "compensating current via shunt inverter" $I_{sh}$is defined.

$$I_{sh} = \sqrt{I_s^2 + I_L^2 - 2I_sI_L\cos(\varphi - \delta)} = I_L\sqrt{1 + cos^2 {}^{\varphi}/_{k^2} - 2\cos\varphi\cos {}^{(\varphi - \delta)}/_{k}} \quad (15)$$

Additionally, as shown in Equations (16) and (17), the shunt inverter controls the harmonic that appears in the load conclusion. Here, I_L^{di} stands for the distortion element, I_L^{fu} for the base element, THD_L for load current's THD, I_{sh}^{di} for the distortion element, I_{sh}^{fu} for the fundamental element and THD_{sh} for shunt inverter current's THD. Consequently, Equation (18) depicts the r.m.s value of the shunt compensatory current.

$$I_L^{di} = I_{sh}^{di} \tag{16}$$

$$THD_L I_L^{fu} = THD_{sh} I_{sh}^{fu} \tag{17}$$

$$I_{sh} = I_{sh}^{fu}\sqrt{1 + THD_{sh}^2} = I_L^{fu}\sqrt{1 + cos^2 {\varphi}/_{k^2} - 2\cos\varphi\cos {(\varphi - \delta)}/_{k} + THD_L^2} \tag{18}$$

As a result, Equation (19) specifies exactly how a shunt inverter's VA rating is defined.

$$SE_{sh} = V_s I_{sh} = V_s I_L^{fu}\sqrt{1 + cos^2 {\varphi}/_{k^2} - 2\cos\varphi\cos {(\varphi - \delta)}/_{k} + THD_L^2} \tag{19}$$

Equations (20) and (21) show how a shunt inverter distributes active and reactive powers.

$$\theta_{sh} = tan^{-1}\{\cos(\varphi - \delta) - \cos\varphi/\sin(\varphi - \delta)\} + 90^o - \delta.$$

Equation (22) specifies the overall reactive power provided by UPQC.

$$P_{sh} = SE_{sh}\cos\theta_{sh} \tag{20}$$

$$QU_{sh} = SE_{sh}\sin\theta_{sh} \tag{21}$$

$$QU_{UPQC} = QU_{se} + QU_{sh} \tag{22}$$

In this case, the placement and dimensions of UPQC on the IEEE 33 bus system and IEEE 69 bus system are offered as encoding to discover the best positioning alternatives for achieving the proposed objectives. In Figure 2, Po_u represents bus line sites where UPQC is to be placed and Q_u UPQC size (reactive power). Here, $u = 1, 2, 3$, and N, where N = 33 and 69, respectively, for the IEEE 33 bus system and IEEE 69 bus systems.

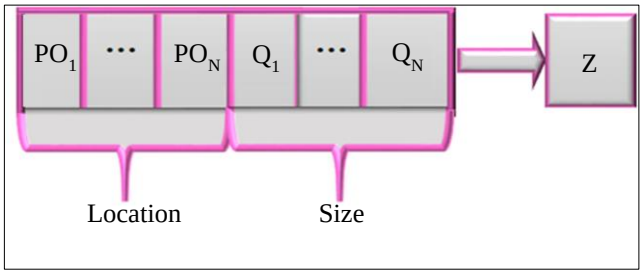

Fig. 2 Solution encoding

The factors taken into consideration that include,

1. $Po_i \leftarrow (1, N]$
2. $Po_i \neq: i, j = 1,2 \ldots., N$

Where, $Q_i \in (Q^{min}, Q^{max})$, Q^{min} and Q^{max} indicates the UPQC optimal boundary. The accepted optimization model, known as HGACDO, is presented with these solutions encoding restrictions in order to achieve the aforementioned goals. The following section provides a detailed description of the proposed Hybrid GA-CDO optimization approach.

2.5. Parameter Optimization Using Hybrid GA-CDO

A novel Hybrid Genetic Algorithm based on Chaotic Dragonfly Optimization (HGACDO) methodology is proposed. This hybridization combines the exploration capabilities of GA) with the efficient global search mechanism of CDO. This integration is unique and tailored to the specific problem of optimal UPQC placement. By combining different optimization techniques, addressing limitations and achieving practical enhancements in power system performance, the research introduces a novel paradigm for power system optimization and further advances the field.

2.5.1. Genetic Algorithm (GA)

The natural selection and genetics theories govern the operation of the GA search algorithm. In GA, a new population is generated by a combination of crossover, mutation probability, selection and preservation of the fittest up until the maximum condition is satisfied. The crossover operations in the GA technique are able to expand by including more than two parents. The search for a possible mating partner is nature's main activity. Several species use various resources not only to advance their collection but also to choose possible companions and develop relationship methods. GA evolution moves on to mutation, where unnerving them causes a solution to change and is subject to change arbitrarily. The efficiency of the solutions the GA has developed is assessed by the fitness function. The expert is able to influence modelling decisions of the fitness function and leads the search as necessary. The finest offspring options need to be selected to be parents in the innovative parental populations to enable converging towards adopting the most advantageous solutions. The total number of fitness values is going to decide the way this selection process becomes effective. There is going to be a selective push regarding better-fit solutions since those with greater fitness require a higher likelihood of selection than those with lower fitness. Termination is defined as the point at which the main evolutionary loop ends. This is applicable in a variety of research contexts. The length of the optimization course is constrained by the cost and time of fitness function computations. The possibility of improving fitness function may be significantly reduced when the optimal value is assessed. If no remarkable behaviour is seen, the evolution process comes to an end.

2.5.2. Chaotic Dragonfly Optimization Algorithm (CDO) Conventional Dragonfly Algorithm

Among the most prominent bio-inspired optimization algorithms is the Dragonfly Algorithm (DA). This algorithm's primary sources of inspiration were the dynamic and static behaviours of dragonfly swarms in nature. Odonata, or dragonflies, are a class of attractive insects, and an example of a tiny predator is the dragonfly. They consume practically all other little insects in nature as food. Additionally, nymph dragonflies consume small fish and many marine insects. Swarm behaviour is determined by three key principles:

1. Separation: This phrase describes avoiding static collisions between individuals. Calculating separation is carried out as follows:

$$S_i = -\sum_{k=1}^{M} Y - Y_k \quad (23)$$

Where$Y$ represents an individual's current location, Y_k represents the location of the k-th neighbour, and M represents an overall amount of neighbours.

2. Alignment: This phrase describes how a person's velocity compares to nearby neighbours. The calculation is as follows:

$$A_i = \frac{\sum_{k=1}^{M} V_k}{M} \quad (24)$$

Where, V_k is the speed of the k-th neighbouring person

3. Cohesion: It refers to people's propensity for the neighbourhood mass centre. This parameter's value is determined as follows:

$$C_i = \frac{\sum_{k=1}^{M} Y_k}{M} - Y \quad (25)$$

4. Interest in a source of food: This parameter measures the separation among the present individual's location and the location of the source food (Y^+), and it is computed as follows:

$$F_i = Y^+ - Y \quad (26)$$

5. Opposed distraction from the external: This is the separation between the current individual's location and the enemy's location (Y), and it is determined as follows:

$$E_i = Y — Y \quad (27)$$

The result of combining these five factors is the behaviour of dragonflies. The searching space's dragonfly locations are modified using the step vector (ΔY) and location vector (Y), two vectors. The following describes a step vector:

$$\Delta Y_{t+1} = (aA_i + sS_i + cC_i + eE_i + fF_i) + \omega \Delta Y_t \quad (28)$$

Where a stands for alignment weight, A_i represents the orientation of the $i-th$ person, s represents separating weight, S_i stands for the division of the $i-th$ person, c is the cohesiveness weight, C_i is the $i-th$ individual's cohesiveness, e is the adversary weight, The location of the adversary of the $i-th$ person is eE_i and food weight is f. F_i is the $i-th$ person's food source, ω is their inertia weight, and the iteration number is represented as *t.*

The overall definition of an individual's location vector is presented as:

$$Y_{t+1} = Y_t + \Delta Y_{t+1} \quad (29)$$

Considering the following variables ($a, s, c, e,$ and f) various exploitative and explorative behaviours are accomplished throughout the optimization process. In simple terms, these variables are employed to maintain an equilibrium among the phases of exploration and exploitation.

During method iterations, the convergence of the dragonfly is ensured owing to the adaptive weighting of the parameters. An optimization process advances and the flying path of dragonflies is equally adjusted. To improve stochastic, randomization, and DA exploration, the application employs a random walk (Le'vy fly). The following definition explains the way dragonflies update their position.

$$Y_{t+1} = Y_t + Le'vy(d) \times Y_t \quad (30)$$

$$Le'vy(y) = 0.01 \times \frac{n_1 \times \sigma}{|n_2|^{\frac{1}{\beta}}} \quad (31)$$

$$\sigma = \left(\frac{\Gamma(1+\beta) \times sin\left(\frac{\pi\beta}{2}\right)}{\Gamma\left(\frac{1+\beta}{2}\right) \times \beta \times 2^{\left(\frac{\beta-1}{2}\right)}} \right)^{1/\beta} \quad (32)$$

Where Γ (x) = (x-1)! d Stands for the location vector's dimension,n_1, n_2 are two random values in the range [0, 1], β is a constant.

Chaotic Dragonfly Algorithm

The changing location of the individuals is influenced by five primary factors in the traditional DA method: alignment, separation, cohesion, interest in a food supply, and distraction from an opponent. However, the initialization of the relevant weights for these five factors is randomized.

This is explained in more detail in the next section; this randomness is capable of having a negative impact on the efficiency and dependability of the method. Chaotic maps are utilized to address these issues, with chaotic values employed in place of the randomized parameters. Chaotic Dragonfly Algorithm (CDA) is a method that combines chaotic maps and dragonfly algorithms.

The updated position in CDA is reconstructed as follows from the definition obtained from (28).

$$\Delta Y_{t+1} = (B(i)A_i + B(i)S_i + B(i)C_i + B(i)E_i + B(i)F_i) + B(i)_{\Delta Y_t} \quad (33)$$

Where$B(i)$ is the result of the $i-th$ iteration's chaotic map. Table 1 displays the beginning parameter values of CDA.

Table 1. CDA parameters

Parameter	Value
Maximum iterations	50
Lower Bound	1
Upper Bound	31
β	1.5
d	31
M	50

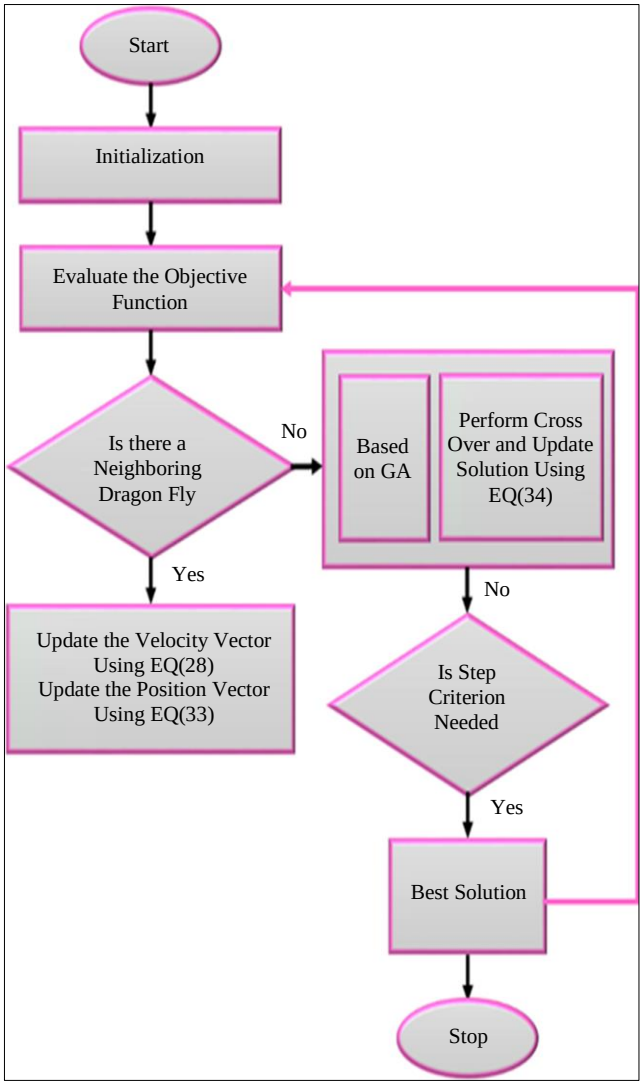

Fig. 3 Flow chart of the proposed HGA-CDA method

2.5.3. Proposed Hybrid GA-CDA

The traditional DA algorithm is a widely recognized optimization method that can potentially be used for improved successful outcomes. It still has a few limitations, including limited accuracy and an insufficient convergence rate.

Therefore, both GA and CDA are combined in the proposed work to solve the aforementioned issues. If the adjacent dragonflies (solutions) have been identified, this proposed approach updates the velocity and location vectors employing Equation (28) and (33) appropriately. As a result, if there are no neighbouring solutions, the crossover GA operation is used to identify children 1 and 2, and the result is revised by averaging the two children as specified by Equation (34). Figure 3 depicts the proposed method's flowchart.

$$Y(t+1) = \frac{Child1+Child2}{2} \quad (34)$$

3. Results and Discussion

In MATLAB, the proposed framework for HGACDA-based UPQC placement optimization is implemented. Here, two different bus systems IEEE 33 and IEEE 69 bus systems are utilized. Depending on where the UPQC was placed, three analyses were conducted: (i) for a single location and (ii) for two locations.

Additionally, by altering the load circumstances to 0%, 50%, 100%, 150%, 200%, and 250%, the evaluation of established work is carried out. For both bus systems, a comparison is done with other traditional approaches, including GA [17], and DA [18], and results have been achieved.

3.1. Convergence Evaluation

This section compares three separate sites' recommended Hybrid GA-CDA-based optimal distribution system positions to those proposed by other models. For each of the three locations, a convergence study for the IEEE 33 bus system is presented in Figure 4.

The convergence analysis shown in Figure 4(a) has shown that the proposed Hybrid GA-CDA model delivers noticeably improved outcomes at the lowest cost when the number of locations is 1. With more iterations, the expense of the function is minimized in this situation. In this instance, the overall cost function for the cost of VSI, power loss, and UPQC appears to be significant at the beginning of the iteration and gradually decreases at the end.

Comparable to this, Figure 4 (b) shows the convergence assessment when there are only two locations. With more iterations, the proposed hybrid GA-CDA model has been demonstrated to provide improved results.

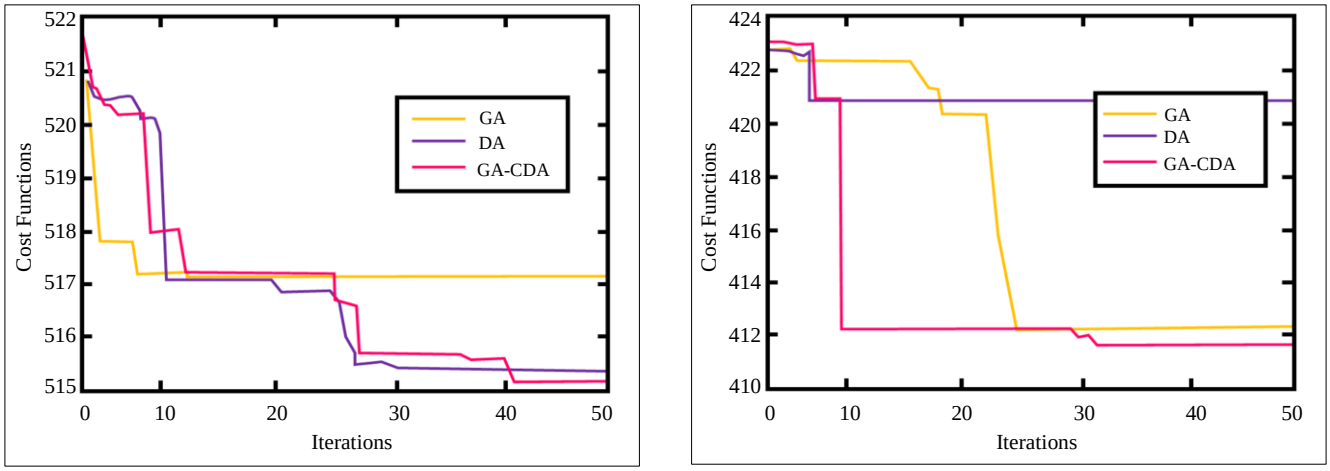

Fig. 4 Convergence analysis of the IEEE 33 bus system using (a) Position=1, and (b) Position=2.

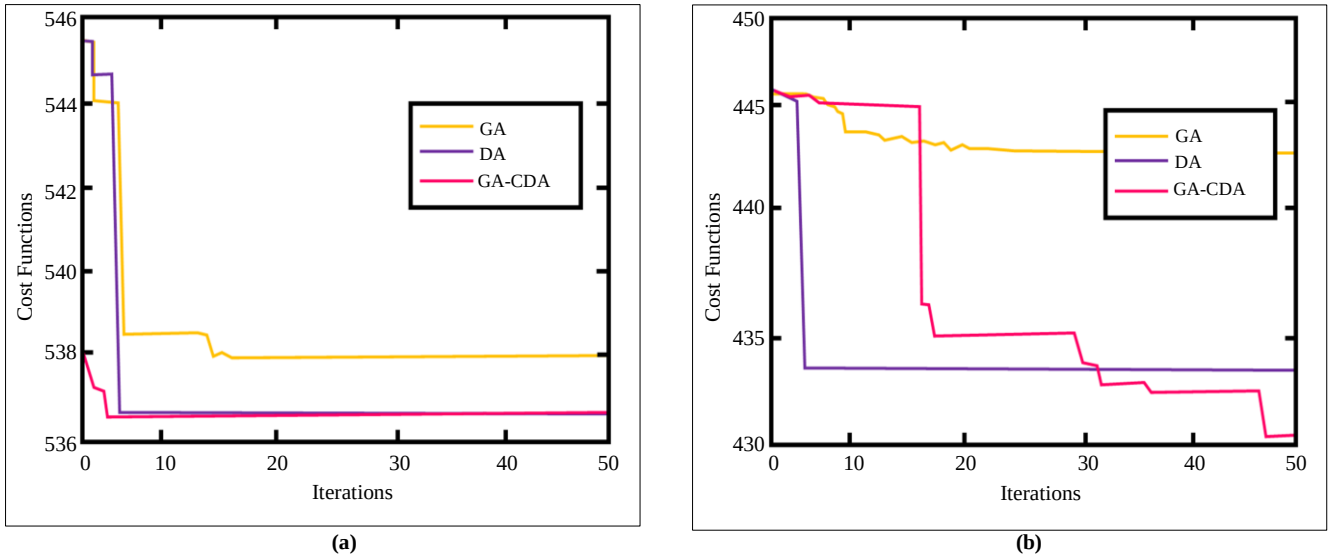

Fig. 5 Convergence analysis of the IEEE 69 bus system using (a) Position=1, and (b) Position=2.

For the IEEE 69 bus system, Figure 5 depicts convergence analysis for the three positions shown in Figures 5 (a) and (b). As a result, the HGACDA technique outperforms traditional systems with slow convergence rates.

Since the recommended model's convergence rate appears too low, an enhancement in power quality becomes possible by the model's proposed positioning and sizing of UPQC in the power system.

3.2. Performance Evaluation

The present section analyses the effectiveness of the proposed HGACDA model, which has been implemented for the IEEE 33 bus and IEEE 69 test bus systems, compared to other conventional methods when location counts (1 and 2) are modified. Table 2 compares the effectiveness of the deployed system to alternative methods for the number of Location 1. The effectiveness assessment of the chosen and alternate choices for the number of locations 1 is shown in Table 2.

Table 2. Effectiveness of the proposed and traditional models when the number of locations and the loading conditions are changed: 1

Loading (%)	GA [17]	DA [18]	GA-CDA (Proposed)
0	518.13	565.12	513.09
50	577.01	586.81	567.67
100	549.95	662.9	598.91
150	662.62	642.83	641.23
200	670.7	620.23	691.09
250	760.78	760.41	740.34

Additionally, Table 3 provides a study that evaluates both the conventional and new methods for the number of Location 2. Similarly, Table 4 specifies the chosen and conventional models used for the investigation's fitness analysis. It has been shown that the overall cost function for different load conditions is accurate, confirming the improvement in power quality of the proposed approach over additional conventional approaches. The efficiency of the proposed HGACDA approach for the IEEE 69 bus system is compared to other methods in Table 5. The evaluation is conducted under two scenarios (1 and 2) by altering the loading circumstances. As a result, Table 5 details the efficiency when there is only one location. The identical findings are presented in Table 6 for the case where the number of places is 2. The specific result shows that, in comparison to earlier models, the model that is chosen achieves a lower fitness value. In the meantime, Table 7 also includes performance evaluation for the two locations in relation to the fitness analysis.

Table 3. Effectiveness of the suggested and traditional models when the loading circumstances are changed in terms of the quantity of locations: 2

Loading (%)	GA [17]	DA [18]	GA-CDA (Proposed)
0	413.34	413.15	410.67
50	484.42	464.37	450.32
100	499.42	532.83	500.78
150	558.13	552.5	534.38
200	598.82	585.53	583.67
250	655.95	668.28	636.55

Table 4. Analysis of overall fitness taking into account proposed and standard models for all three sites (1 and 2)

			GA [17]	DA [18]	GA-CDA (Proposed)
Single objective	VSI	Locations-1	33.987	33.788	33.542
		Locations-2	30.378	30.386	30.756
	$UPQC_{cost}$	Locations-1	192.56	192.41	201.22
		Locations-2	108.04	107.44	108.24
	P_{Loss}	Locations-1	288.8	288.88	282.28
		Locations-2	27373	273.92	281.20
Multi-objective	Final Fitness(OB)	Locations-1	515.34	515.08	517.10
		Locations-2	412.15	411.74	420.22

Table 5. Effectiveness of the proposed and traditional models when a number of locations and the loading conditions are changed: 1

Loading (%)	GA [17]	DA [18]	GA-CDA (Proposed)
0	556.64	546.64	545.62
50	589.34	559.34	536.23
100	573.4	573.42	560.4
150	590.07	590.07	579.06
200	600.64	599.61	587.60
250	628.13	684.11	615.11

Table 6. Effectiveness of the proposed and conventional approaches when the number of locations and conditions for loading are modified:2

Loading (%)	GA [17]	DA [18]	GA-CDA
0	442.96	443.2	429.31
50	455.8	464.11	444.50
100	469.55	471.41	445.12
150	485.15	484.92	470.40
200	493	498.22	490.32
250	516.24	523.09	512.3

Table 7. Analysis of overall fitness using proposed and traditional techniques for all three locations (1 and 2)

			GA [17]	DA [18]	GA-CDA (Proposed)
Single objective	VSI	Locations-1	22.331	22.36	22.324
		Locations-2	22.063	21.967	19.260
	$UPQC_{cost}$	Locations-1	183.36	183.36	183.33
		Locations-2	104.32	108.45	107.2
	P_{Loss}	Locations-1	330.96	330.96	330.91
		Locations-2	306.58	302.79	303.58
Multi-objective	Final Fitness(OB)	Locations-1	536.64	536.64	536.60
		Locations-2	432.14	433.2	430.28

4. Conclusion

The proposed approach takes advantage of the coordination of an HGACDO to discover the optimum and efficient places for UPQC placement. The GA delivers its strong exploration capacities, replicating natural selection to refine alternative solutions. This integrates with the CDO rapid global search technique, which is motivated by cuckoo brood parasitism behaviour. This synergy culminates in the HGACDO approach, which is specifically optimized for efficient UPQC allocation. The proposed approach considers not only the technical complexities of UPQC installation but also the cost-effectiveness, voltage stability index and power losses. HGACDO algorithm enhances the accuracy of UPQC positioning by merging GA and CDO. A thorough evaluation of benchmark IEEE 69 and IEEE 33 test bus systems is performed to confirm the efficacy of the HGACDO model. The results show considerable power quality, stability, and operating efficiency gains. Thus, the improved power quality provided by the proposed method will enable the proper positioning and sizing of UPQC in power systems.

References

[1] Khalil Gholami, Shahram Karimi, and Ehsan Dehnavi, "Optimal Unified Power Quality Conditioner Placement and Sizing in Distribution Systems Considering Network Reconfiguration," *International Journal of Numerical Modelling: Electronic Networks, Devices and Fields*, vol. 32, no. 1, 2019. [CrossRef] [Google Scholar] [Publisher Link]

[2] Kaladhar Gaddala, and P. Sangameswara Raju, "Enhanced Self-Adaptive Bat Algorithm for Optimal Location of Unified Power Quality Conditioner," *Journal of Computational Mechanics, Power System and Control*, vol. 2, no. 3, pp. 28-38, 2019. [CrossRef] [Google Scholar] [Publisher Link]

[3] H.R. Sukhesh, U. Senthil Vadivu, and B.K. Keshavan, "Optimal Placement of Fuzzy Based Nonal Switched UPQC Topology with Distributed Generation for the Power Quality Enhancement in IEEE 14 Bus System," *Power Research-A Journal of CPRI*, vol. 15, no. 1, pp. 1-6, 2019. [CrossRef] [Google Scholar] [Publisher Link]

[4] M.L. Ramanaiah, and M.D. Reddy, "Optimal Placement of Unified Power Quality Conditioner Using Ant Lion Optimization Method," *International Journal of Applied Engineering Research*, vol. 12, no. 13, pp. 3708-3713, 2017. [Google Scholar] [Publisher Link]

[5] Hossein Shayeghi et al., "Sizing and Placement of DG and UPQC for Improving the Profitability of Distribution System Using Multi-objective WOA," *International Conference on Intelligent Systems Design and Applications*, Auburn, WA, USA, pp. 810-820, 2019. [CrossRef] [Google Scholar] [Publisher Link]

[6] Umar Musa et al., "Implementation of Bacterial Foraging Algorithm Based Model for UPQC Placement in a Practical Distribution Feeder," *Covenant Journal of Engineering Technology*, vol. 4, no. 1, pp. 2682-5317, 2020. [CrossRef] [Google Scholar] [Publisher Link]

[7] Shubh Lakshmi, and Sanjib Ganguly, "An On-Line Operational Optimization Approach for Open Unified Power Quality Conditioner for Energy Loss Minimization of Distribution Networks," *IEEE Transactions on Power Systems*, vol. 34, no. 6, pp. 4784-4795, 2019. [CrossRef] [Google Scholar] [Publisher Link]

[8] Lakshminarayana Gadupudi et al., "Fuzzy-based Fifteen-Level VSC for STATCOM Operations with Single DC-Link Voltage," *Sustainability*, vol. 15, no. 7, pp. 2-15, 2023. [CrossRef] [Google Scholar] [Publisher Link]

[9] L. Narayana Gadupudi et al., "Seven Level Voltage Source Converter Based Static Synchronous Compensator with A Constant DC-Link Voltage," *Applied Sciences*, vol. 11, no. 16, pp. 2-17, 2021. [CrossRef] [Google Scholar] [Publisher Link]

[10] Kondreddi Saicharan, and Atma Ram Gupta, "Effective Placement of UPQC and DG in Radial Distribution System," *1st IEEE International Conference on Measurement, Instrumentation, Control and Automation*, pp. 1-6, 2020. [CrossRef] [Google Scholar] [Publisher Link]

[11] Xiaoguang Zhu et al., "Optimal Location and Capacity Planning of UPQCS Considering Operation Dispatching in Distribution Grid with Distributed Generators," *Energy Reports*, vol. 8, pp. 832-842, 2022. [CrossRef] [Google Scholar] [Publisher Link]

[12] L. Narayana Gadupudi, and Gudapati Sambasiva Rao, "7-Level Transformers Integrated Voltage Source Converter Based STATCOM for Voltage Profile Enhancement," *Solid State Technology*, vol. 63, no. 5, pp. 3134-3141, 2020. [Google Scholar] [Publisher Link]

[13] Y. Priyanka, and Raghu Ram, "Performance Analysis of Distribution System with Optimal Allocation of Unified Power Quality Conditioner Considering Distribution Network Reconfiguration," *International Journal of Intelligent Engineering & Systems*, vol. 16, no. 1, pp. 364-374, 2023. [CrossRef] [Google Scholar] [Publisher Link]

[14] Khadija A.l. Balushi, "Optimal Location and Sizing of UPQC for Improving Power System Quality," *Journal of Computational Mechanics, Power System and Control*, vol. 3, no. 2, pp. 26-32, 2020. [CrossRef] [Google Scholar] [Publisher Link]

[15] Amal Amin et al., "Optimal Placement of Distribution Static Compensators in Radial Distribution Systems Using Hybrid Analytical-Coyote optimization Technique," *21st International Middle East Power Systems Conference*, Cairo, Egypt, pp. 982-987, 2019. [CrossRef] [Google Scholar] [Publisher Link]

[16] M. Laxmidevi Ramanaiah, and M. Damodar Reddy, "Moth Flame Optimization Method for Unified Power Quality Conditioner Allocation," *International Journal of Electrical and Computer Engineering*, vol. 8, no. 1, pp. 530-537, 2018. [CrossRef] [Google Scholar] [Publisher Link]

[17] J.R. Fernández et al., "A Genetic Algorithm for the Characterization of Hyperelastic Materials," *Applied Mathematics and Computation*, vol. 329, pp. 239-250, 2018. [CrossRef] [Google Scholar] [Publisher Link]

[18] Mohammad Jafari, and Mohammad Hossein Bayati Chaleshtari, "Using Dragonfy Algorithm for Optimization of Orthotropic Infinite Plates with A Quasi-Triangular Cut-Out," *European Journal of Mechanics - A/Solids*, vol. 66, pp. 1-14, 2017. [CrossRef] [Google Scholar] [Publisher Link]